Spin Hall Effect in Disordered Organic Solids

Z. G. Yu
ISP/Applied Sciences Laboratory, Washington State University, Spokane, Washington 99210, USA
(Received 25 March 2015; published 6 July 2015)

We study the spin Hall effect (SHE) in disordered π-conjugated organic solids, where individual molecules are oriented randomly and electrical conduction is via carrier hopping. The SHE, which arises from interference between direct ($i \to j$) and indirect ($i \to k \to j$) hoppings in a triad consisting of three molecules i, j, and k, is found to be proportional to $\lambda(\boldsymbol{n}_i \times \boldsymbol{n}_j + \boldsymbol{n}_j \times \boldsymbol{n}_k + \boldsymbol{n}_k \times \boldsymbol{n}_i)$, where λ is the spin admixture of π electrons due to the spin-orbit coupling and $\boldsymbol{n}_i$ is the orientation vector of molecule i. Electrical conductivity σ_{qq} ($q = x, y, z$) and spin Hall conductivity $\sigma_{\rm sh}$ are computed by numerically solving the master equations of a system containing $32 \times 32 \times 32$ molecules and summing over contributions from all triads in the system. The obtained value of the spin Hall angle $\Theta_{\rm sh}$ is consistent with experimental data in PEDOT:PSS, with a predicted temperature dependence of $\log \Theta_{\rm sh} \sim T^{-1/4}$.

DOI: 10.1103/PhysRevLett.115.026601 PACS numbers: 72.25.Dc, 71.70.Ej, 72.20.Ee, 72.80.Le

The spin Hall effect (SHE), which enables a direct conversion between an electric field and spin current [1], is a fundamental material property critical to spintronic applications and has been intensively studied in inorganic materials in the last decade [2]. Recently the (inverse) SHE has been successfully detected in organic devices, opening an arena for manipulation and detection of pure spin current [3,4] in organic spintronics [5,6], a rapidly growing field motivated by the weak spin-orbit couplings (SOCs) and hyperfine interactions (HFIs) in organics [7]. While the SHE is adequately understood in crystalline inorganic materials, little is known about the SHE in disordered organic solids, where electrical conduction is via electron hopping. The few theoretical works on the SHE in the hopping regime [8,9] are confined to the Dresselhaus [10] and Rashba [11] forms of SOC, which are suitable for crystalline inorganic semiconductors but become inapplicable to the organics. Furthermore, in these works, the SHE appears only at the second order of SOC [8,9], which would render the SHE too weak to be detected in organics. Here, using the newly developed understanding of SOC in organics [12], we derive the SHE in disordered π-conjugated organic solids. It is found that the SHE originates from misaligned orientations of π-conjugated molecules in a triad and is present at the first order of SOC. The spin Hall conductivity and electrical conductivity, obtained by exactly solving the master equations in a large system, are consistent with experiment. Our work suggests that the SHE in organic solids may be tunable by controlling their morphology.

The organic materials used in devices are π-conjugated molecules or oligomers in the form of dense films. The sp^2 hybridization in a π-conjugated molecule results in its planar structure, whose orientation can be characterized by the vector normal to the molecular plane, $\boldsymbol{n}_i = (\sin\theta_i \cos\phi_i, \sin\theta_i \sin\phi_i, \cos\theta_i)^T$, with (θ_i, ϕ_i) being the corresponding polar and azimuthal angles. The dense-film form implies that the orientations of these molecules are not identical. In the presence of SOC, the eigenstates of π electrons in molecule i are not pure spin states and must contain spin (and orbital) mixing [12],

$$|i_{+(-)}\rangle = |p_{i\tilde{z}}\uparrow(\downarrow)\rangle + \frac{\xi}{2\Delta}[-(+)i\sin\theta_i|p_{i\tilde{y}}\uparrow(\downarrow)\rangle + (-)e^{+(-)i\phi_i}|p_{i\tilde{x}}\downarrow(\uparrow)\rangle + i\cos\theta_i e^{+(-)i\phi_i}|p_{i\tilde{y}}\downarrow(\uparrow)\rangle].$$

Here the subscript $+(-)$ denotes the predominant spin orientation of the state being parallel (antiparallel) to the spin-quantization axis, which is fixed at the z axis throughout the paper. $p_{i\tilde{q}}$ ($q = x, y, z$) are the p orbitals in the local coordinates so that $p_{i\tilde{z}}$ always represents the π orbital and $p_{i\tilde{x}(\tilde{y})}$ represent σ orbitals, ξ is the atomic SOC, and Δ is the energy splitting between π and σ orbitals. For a π electron hopping from molecule i with orientation $\boldsymbol{n}_i$ to molecule j with orientation $\boldsymbol{n}_j$, the hopping amplitude $\langle j_\pm|V|i_\pm\rangle \equiv \hat{V}_{ji}$ can be expressed in the 2×2 spin space as (see Supplemental Material Ref. [13])

$$\hat{V}_{ji} = \sum_{q=x,y,z}\left[n_i^q n_j^q v_{ji}^q \hat{1} - i\frac{\xi}{2\Delta}\hat{\sigma}_q e_{quv} n_i^u n_j^v (v_{ji}^u + v_{ji}^v)\right], \quad (1)$$

where $\hat{1}$ is the unit matrix, $\hat{\sigma}_q$ the Pauli matrix, e_{quv} the antisymmetric unit tensor of rank three, and v_{ji}^q the hopping integral between two p orbitals at molecules i and j with their orientations both along the q axis. By assuming $v_{ji}^x = v_{ji}^y = v_{ji}^z = V_{ji}^0$, Eq. (1) becomes $\hat{V}_{ji} = V_{ji}^0[\boldsymbol{n}_i \cdot \boldsymbol{n}_j\hat{1} - i\lambda\hat{\boldsymbol{\sigma}} \cdot (\boldsymbol{n}_i \times \boldsymbol{n}_j)]$ with $\lambda = \xi/\Delta$. In a densely packed organic solid, the molecular-orientation variation among neighboring molecules should be gradual (i.e., small angle θ_{ij} between $\boldsymbol{n}_i$ and $\boldsymbol{n}_j$) to avoid an otherwise large steric force [14]. Since $\boldsymbol{n}_i \cdot \boldsymbol{n}_j \simeq 1 - \theta_{ij}^2/2$ and $\boldsymbol{n}_i \times \boldsymbol{n}_j \simeq \theta_{ij}$, to the first order of θ_{ij}, $\hat{V}_{ji}$ is approximately

$$\hat{V}_{ji} \simeq V_{ji}^0[\hat{1} - i\lambda\hat{\boldsymbol{\sigma}}\cdot(\boldsymbol{n}_i\times\boldsymbol{n}_j)] \simeq V_{ji}^0 e^{-i\lambda\boldsymbol{\sigma}\cdot(\boldsymbol{n}_i\times\boldsymbol{n}_j)}. \quad (2)$$

Equation (2) indicates that because of the SOC and misalignment of π orbitals among different molecules, an electron attains an additional phase shift after each hop. This phase shift, to the first order of SOC, does not alter the hopping probability between two sites (a bond), $\hat{V}_{ij}\hat{V}_{ji} = V_{ij}^0 V_{ji}^0$, but will manifest itself in a triad, whose importance in the hopping transport was first recognized by Holstein when studying the Hall effect [15]. The product of three hopping integrals over a triad loop contains a net phase shift,

$$\hat{V}_{ik}\hat{V}_{kj}\hat{V}_{ji} = V_{ik}^0 V_{kj}^0 V_{ji}^0(\hat{1} - i\lambda\hat{\boldsymbol{\sigma}}\cdot\boldsymbol{N}_{ijk}). \quad (3)$$

Geometrically, $\boldsymbol{N}_{ijk} \equiv \boldsymbol{n}_i\times\boldsymbol{n}_j + \boldsymbol{n}_j\times\boldsymbol{n}_k + \boldsymbol{n}_k\times\boldsymbol{n}_i$ is twice the area of a triangle with its vertices on the surface of a unit sphere (Fig. 1), and it is finite when the molecular orientations in a triad are different from one another, as in a disordered organic solid. On the other hand, when the π orbitals are all aligned, $\boldsymbol{N}_{ijk}$ vanishes and so does the SHE. We emphasize that it is this misalignment of π orbitals that unveils the SHE at the first order of SOC, a physics not captured before. Hence, the SHE in organics may be tuned by controlling the degree of molecular alignment during the film growth or deposition process. It should be noted that the HFI, another important interaction influencing spin dynamics in organics, cannot give rise to the SHE because the HFI does not affect the hopping integral and causes no interference among different electron paths [16,17].

Hopping electrical transport can be understood by studying the change of real-space electron distribution in the presence of external fields. Since the SHE involves spin current, we express the general electron distribution at site i as $\hat{f}_i = f_i^{\rm c}\hat{1} + \hat{\sigma}_z f_i^{\rm s}$, with $f_i^{\rm c}$ ($f_i^{\rm s}$) being the charge (spin) density and the spin-quantization axis along the z axis. In equilibrium, the system is nonmagnetic and $\hat{f}_i = f_i^0\hat{1} \equiv [1 + e^{\beta(\epsilon_i-\mu)}]^{-1}\hat{1}$, where ϵ_i is the electron energy at site i, μ the Fermi level, and $\beta = 1/k_BT$, with k_B and T being the Boltzmann constant and temperature. In the presence of an electric field, the dynamic of $\hat{f}_i$ is described by the master equation,

$$\frac{d\hat{f}_i}{dt} = \sum_j\Big\{\hat{f}_j(1-\hat{f}_i)\Big[w_{ji} + \sum_k(1-\hat{f}_k)\hat{\sigma}_z w_{jki}^{\rm e}\Big] - \hat{f}_i(1-\hat{f}_j)\Big[w_{ij} + \sum_k\hat{f}_k\hat{\sigma}_z w_{jki}^{\rm h}\Big]\Big\}, \quad (4)$$

where w_{ij} is the direct electron hopping probability from sites i to j or, equivalently, the direct hole hopping from j to i, and $w_{jki}^{\rm e(h)} \propto \lambda N_{jki}^z$ is the indirect hopping probability from j to i for the electron (hole) through an intermediate site k. The first (second) term on the right-hand side of Eq. (4) is the total electron (hole) hopping from j to i. For generality, the applied electric field has a finite frequency ω, and the dc transport properties can be obtained in the limit $\omega \to 0$.

In the linear-response regime, the change in electron distribution, $\delta\hat{f}_i \equiv \hat{f}_i - f_0\hat{1}$, is small and can be characterized by a deviation in its electrochemical potential from the Fermi level μ in equilibrium, $\delta\hat{\mu}_i$,

$$\delta\hat{f}_i = \beta f_i^0(1-f_i^0)\delta\hat{\mu}_i \equiv \beta f_i^0(1-f_i^0)(\delta\mu_i^{\rm c} + \hat{\sigma}_z\mu_i^{\rm s}). \quad (5)$$

The electric field affects the hopping via $w_{ji}/w_{ji}^0 = w_{jik}^{\rm e}/w_{jik}^{\rm e0} = w_{jik}^{\rm h0}/w_{jik}^{\rm h} = 1 - \beta e\boldsymbol{E}\cdot(\boldsymbol{R}_j - \boldsymbol{R}_i)/2$, where w_{ji}^0, $w_{jki}^{\rm e0}$, and $w_{jik}^{\rm h0}$ are the values w_{ji}, $w_{jki}^{\rm e}$, and $w_{jik}^{\rm h}$ in equilibrium, and $\boldsymbol{R}_i$ gives the coordinates of site i. Accordingly, the master equations in Eq. (4) reduce to coupled linear equations of $\delta\mu_i^{\rm c}$ and $\mu_i^{\rm s}$,

$$i\omega C_i\frac{\mu_i^{\rm s}}{e} = \sum_j\frac{\mu_j^{\rm s} - \mu_i^{\rm s}}{eZ_{ij}} + e^2\beta\sum_{jk}V_j W_{jki}^z, \quad (6)$$

$$i\omega C_i\frac{\delta\mu_i^{\rm c}}{e} = \sum_j\frac{V_j - V_i}{Z_{ij}} + e\beta\sum_{jk}\mu_j^{\rm s}W_{jki}^z. \quad (7)$$

Here $V_i = \delta\mu_i^{\rm c}/e - \boldsymbol{E}\cdot\boldsymbol{R}_i$, $C_i = e^2\beta f_i^0(1-f_i^0)$, $Z_{ij}^{-1} = e^2\beta f_i^0(1-f_j^0)w_{ij}^0 = e^2\beta f_j^0(1-f_i^0)w_{ji}^0$, which is symmetric under the interchange of i and j, and the effective three-site hopping probability,

$$W_{jki}^z \equiv f_j^0(1-f_i^0)(1-f_k^0)w_{jki}^{\rm e0} + (1-f_j^0)f_i^0 f_k^0 w_{jki}^{\rm h0}, \quad (8)$$

is antisymmetric under the interchange of any pair of subscripts. Once the solutions $\mu_i^{\rm s}$ and $\delta\mu_i^{\rm c}$ are found, the spin current is evaluated according to its definition,

$$\boldsymbol{j}^{\rm s} \equiv \frac{e}{\Omega}\sum_i\boldsymbol{R}_i\frac{df_i^{\rm s}}{dt} = \frac{i\omega}{\Omega e}\sum_i\boldsymbol{R}_i C_i\mu_i^{\rm s}, \quad (9)$$

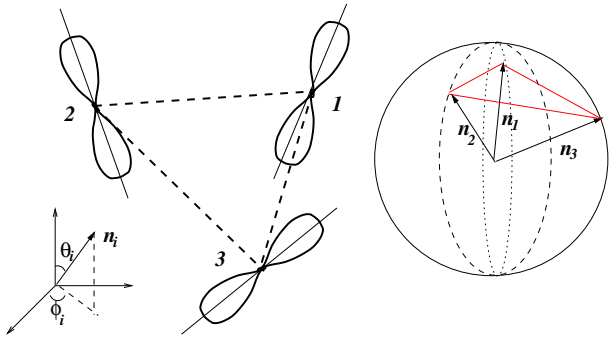

FIG. 1 (color online). Triad with three molecules oriented along $\boldsymbol{n}_i$ ($i = 1, 2, 3$). The SHE is proportional to $\boldsymbol{N}_{123}/2$, the area of the triangle formed by (θ_i,ϕ_i) on a unit sphere.

with Ω being the volume of the system, and the spin-Hall conductivity can be obtained via $\sigma_{\rm sh} = j_y^{\rm s}/E$, with $j_y^{\rm s}$ being the y component of $\boldsymbol{j}^{\rm s}$ and $\boldsymbol{E}$ along the x axis.

Equations (6) and (7) reveal the key role played by the three-site hopping W_{jkl}^z in both the SHE and ISHE. Through W_{jkl}^z, a change in V_i due to an applied electric field can result in a change in spin distribution $\mu_i^{\rm s}$ and therefore a spin current, i.e., the SHE, and conversely, a change in $\mu_i^{\rm s}$, can lead to a change in $\delta\mu_i^{\rm c}$ or an electric motive force, i.e., the ISHE.

To reliably calculate the dc SHE in a disordered system, proper summation and average over a large system are essential. In the literature of the hopping Hall effect, the common approach is to identify "representative" triads that control the overall properties of the entire system [18], which involves uncontrollable approximations. Here, instead, we numerically solve the master equations exactly in a sufficiently large system, which is conceptually simple with a guaranteed accuracy. For a system consisting of $\mathcal{N}$ molecules, Eqs. (6) and (7) have approximately $2\mathcal{N}$ equations, which can be reduced to two sets of $\mathcal{N}$ equations if the three-site hopping is treated as a perturbation. We can then solve Eq. (7) without the three-site terms and denote the obtained solution as V_i^{0x} and V_i^{0y} for $\boldsymbol{E}$ along the x and y axes, respectively. The solution to Eq. (6) after W_{ijk}^z is included can be written as $\mu_i^{\rm s} = e^2\beta\sum_{jkl}[(g+i\omega c)^{-1}]_{ij}V_j^{0x}W_{jkl}^z$, where matrices $g_{ij} \equiv Z_{ij}^{-1} - \delta_{ij}\sum_k Z_{ik}^{-1}$ and $c_{ij} \equiv C_i\delta_{ij}$. Since y_i is related to V_i^{0y} via $y_i = (i\omega E)^{-1}C_i^{-1}(g+i\omega c)_{ij}V_j^{0y}$, the spin current $j_y^{\rm s}$ in Eq. (9) is $j_y^{\rm s} = i\omega(\Omega E)^{-1}\sum_i y_i C_i \mu_i^{\rm s} = -\beta e^2(\Omega E)^{-1}\sum_{jki} W_{jki}^z V_j^{0y} V_i^{0x}$. Using the antisymmetric property of W_{ijk}^z, $\sigma_{\rm sh}$ can be expressed as

$$\sigma_{\rm sh} = -\frac{e^2\beta}{6\Omega E^2}\sum_{ijk} W_{ikj}^z[(\boldsymbol{V}_i^0 - \boldsymbol{V}_k^0)\times(\boldsymbol{V}_k^0 - \boldsymbol{V}_j^0)]_z, \quad (10)$$

where the projections of $\boldsymbol{V}_i^0$ on the q axis give the electrochemical potentials for the case when the external field $\boldsymbol{E}$ is directed along the q axis. This expression generalizes that due to Butcher and Kumar for calculating the Hall mobility [19]. Note that Eq. (10) is independent of ω and can therefore be used to calculate the dc SHE, in which $\boldsymbol{V}_j^0$ is the solution to $0 = \sum_j Z_{ij}^{-1}(\boldsymbol{V}_j^0 - \boldsymbol{V}_i^0)$ with a dc bias applied along the corresponding axes. The obtained $\boldsymbol{V}_i^0$ can also be used to evaluate the dc electrical conductivity of the system via [19]

$$\sigma_{qq} = \frac{1}{2\Omega E^2}\sum_{ij} Z_{ij}^{-1}(V_i^{0q} - V_j^{0q})^2. \quad (11)$$

Experimentally the organic material where the ISHE was first observed is poly(3,4-ethylenedioxythiophene): poly(styrenesulfonate) (PEDOT:PSS) [3]. The $I-V$ characteristics of this material are found to be linear [3], indicating that the electrical conductivity is independent of bias and that carriers must exist before a bias is applied. Thus, the system should have a large density of states near the Fermi level. Moreover, the measured temperature dependence of the conductivity in PEDOT:PSS [20] follows the Mott's variable range hopping (VRH), $\log\sigma_{xx} \sim T^{-1/4}$, through an impurity band [21]. The impurity-band transport was also proposed to explain many properties of charge and spin transport in organic spintronic devices [22]. In addition, recent experimental and theoretical studies [23,24] suggest that bipolaron formation in PEDOT is unimportant. This evidence suggests that the hopping probability in PEDOT:PSS has the Miller-Abrahams form [25], where electron-phonon coupling is treated perturbatively,

$$Z_{ij}^{-1} = \nu e^{-2\alpha R_{ji}} e^{-(\beta/2)(|\epsilon_i-\mu|+|\epsilon_j-\mu|+|\epsilon_{ji}|)}. \quad (12)$$

Here the hopping integral V_{ji}^0 is assumed to exponentially decay with the hopping distance $R_{ji} = |\boldsymbol{R}_j - \boldsymbol{R}_i|$, $V_{ji}^0 = V_0 e^{-\alpha R_{ji}}$, with α^{-1} being the localization length of π-electron wave functions in the molecules, $\epsilon_{ji} = \epsilon_j - \epsilon_i$, and $\nu = \pi V_0^2\bar{\gamma^2}/\hbar^2$ with $\bar{\gamma^2}$ depending only on the electron-phonon coupling γ and phonon properties. By using the same weak electron-phonon approximation, the three-site hopping probability (see Supplemental Material Ref. [13]) is

$$W_{jki}^z = \frac{\lambda N_{jki}^z}{V_0}\hbar\nu^2 e^{-\alpha(R_{jk}+R_{ki}+R_{ij})}\left[\exp\left(-\frac{\beta}{2}(|\epsilon_j-\mu| + |\epsilon_k-\mu| + |\epsilon_{ji}| + |\epsilon_{ki}|)\right) + i\rightleftharpoons j + i\rightleftharpoons k\right]. \quad (13)$$

In our numerical calculations, the system consists of $32\times32\times32$ molecules forming a cubic lattice with a lattice constant of a. The site energy ϵ_i is uniformly distributed in the interval $[-\epsilon_0/2, \epsilon_0/2]$, reflecting the disordered environment of the molecules, and the Fermi level μ in equilibrium is set to zero; i.e., the system has a finite density of state at the Fermi level, as in PEDOT:PSS. αa is fixed at 2; i.e., the electron wave functions can extend to neighboring sites, consistent with the relatively delocalized wave functions observed from infrared-absorption spectra [26]. Since the measured electrical transport in PEDOT:PSS is anisotropic, this isotropic lattice should be regarded as an "averaged" structure of PEDOT:PSS, with the electrical conductivity being the geometric mean of two conductivities along the x and y axes. The SOC parameter λ is estimated as 10^{-3}, from the value of T_6, which has a very similar structure as PEDOT [12]. Individual molecular orientations are random. Hopping between any bond (i,j) and among any triad (i,j,k), Z_{ij}^{-1} and W_{jki}^z in Eqs. (12) and (13), in the entire lattice is

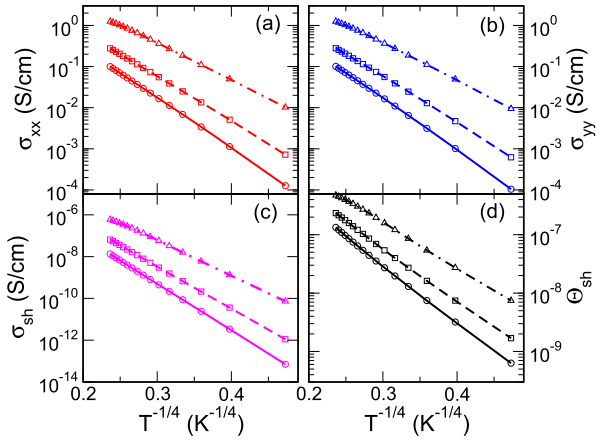

FIG. 2 (color online). Electrical conductivity σ_{xx} (a) and σ_{yy} (b), spin Hall conductivity σ_{sh} (c), and spin Hall angle Θ_{sh} (d) as a function of $T^{-1/4}$ for different values of energy disorder ϵ_0. Solid, dashed, and dot-dashed lines correspond to $\epsilon_0 = 0.6$, 0.4, and 0.2 eV, respectively. The parameters are $\alpha a = 2$, $\lambda = 10^{-3}$, $\nu = 3 \times 10^{11}$ s^{-1}, and $V_0 = 0.1$ eV.

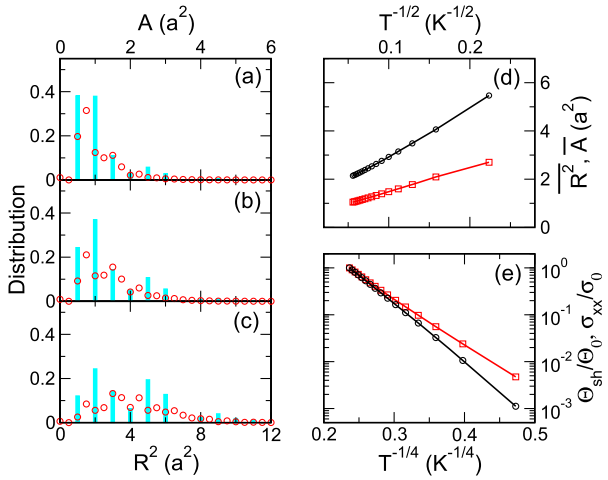

FIG. 3 (color online). $D(R^2)$ (bars) and $D(A)$ (circles) for $T = 300$ (a), 120 (b), and 40 K (c). (d) $\overline{R^2}$ (circles) and $\bar{A}$ (squares) as a function of $T^{-1/2}$. (e) Comparison of temperature dependences in Θ_{sh} (squares) and σ_{xx} (circles). σ_0 and Θ_0 are the values of σ_{xx} and Θ_{sh} at $T = 320$ K. The energy disorder is $\epsilon_0 = 0.6$ eV. Other parameters are as in Fig. 2.

allowed. Hence, possible VRH is automatically included. Nevertheless, the exponential decay in wave functions allows us to introduce a cutoff in the hopping distance, beyond which the hopping integral can be neglected. Such a cutoff facilitates application of sparse-matrix techniques in solving the master equations.

Figure 2 shows the calculated electric conductivity along different directions, σ_{xx} and σ_{yy}, the spin Hall conductivity σ_{sh}, and the spin Hall angle, $\Theta_{sh} \equiv \sigma_{sh}/(\sigma_{xx}\sigma_{yy})^{1/2} = \sigma_{sh}/\sigma_{qq}$ [27], as a function of temperature for different energy disorders, measured by ϵ_0. It is seen that σ_{xx} and σ_{yy} are virtually identical for various disorder strengths, indicating that the system is sufficiently large and that the numerical results are both convergent and reliable. The logarithm of σ_{qq}, when plotted vs $T^{-1/4}$, is linear over a large temperature range, meaning that electrical transport in the system is indeed VRH. At room temperature, $\Theta_{sh} \sim 10^{-7}$, in good agreement with the measured value, and $\sigma_{qq} \sim 0.1$–1 S/cm, close to the geometric mean of measured conductivities, 1.6×10^{-3} and 660 S/cm along the x and y axes [3]. In addition, we see that $\log(\sigma_{sh}, \Theta_{sh}) \sim T^{-1/4}$ and that as the disorder strength increases, the temperature dependences in σ_{qq}, σ_{sh}, and Θ_{sh} are enhanced.

Figure 3, which displays distributions of the square of hopping distance $D(R^2)$ and triad area $D(A)$ at different temperatures, further illuminates the VRH nature in this system. The distributions are measured as $D(R^2) = \sum_{ij}|I_{ij}(R_{ij}^2 = R^2)|/\sum_{ij}|I_{ij}|$, where $I_{ij} = Z_{ij}^{-1}(V_i^{0q} - V_j^{0q})$, and $D(A) = \sum_{ijk}|W_{ijk}^z(A_{ijk} = A)|/\sum_{ijk}|W_{ijk}|$, where A_{ijk} is the area of the triad (i, j, k). We see that as the temperature decreases, distributions $D(R^2)$ and $D(A)$ become broader and the peaks shift toward the larger values. The averaged values, $\overline{R^2} \equiv \sum R^2 D(R^2)$ and $\bar{A} \equiv \sum A D(A)$, are both proportional to $T^{-1/2}$, as shown in Fig. 3(d), consistent with the VRH. The temperature dependence of Θ_{sh}, according to Fig. 3(e), is weaker than that of σ_{xx}.

The numerical results on σ_{sh} and Θ_{sh} can be understood from Mott's theory, where the conductance

$$Z^{-1} \sim \exp\left[-2\alpha r - \frac{\epsilon_0 a^3}{(4\pi r^3/3)k_B T}\right] \tag{14}$$

reaches a maximum at the most probable hopping distance, $\bar{r} = [9\epsilon_0 a^3/(8\pi\alpha k_B T)]^{1/4}$, and accordingly $\sigma_{xx} \sim (Z^{-1})_{\max} \sim e^{-8\alpha\bar{r}/3} = e^{-(T_0/T)^{1/4}}$ with $T_0 = 512(\alpha a)^3\epsilon_0/(9\pi k_B)$. This expression of T_0 would give a value of 1.0×10^6 K for $\epsilon_0 = 0.6$ eV and $\alpha a = 2$, which is close to the value of 1.6×10^6 K, from fitting the results in Fig. 2 into $\sigma_{qq} \sim \exp[-(T_0/T)^{-1/4}]$. Both values are similar to the experimental value of 3×10^6 in a PEDOT:PSS system [20]. Expressing Eq. (13) as

$$W^z \sim \exp\left[-3\alpha r - \frac{2\epsilon_0 a^3}{(4\pi r^3/3)k_B T}\right], \tag{15}$$

and substituting r by $\bar{r}$, we estimate σ_{sh} and Θ_{sh} as

$$\sigma_{sh} \sim W^z \sim e^{-13\alpha\bar{r}/3}, \qquad \Theta_{sh} = \frac{\sigma_{sh}}{\sigma_{qq}} \sim e^{-5\alpha\bar{r}/3}. \tag{16}$$

Since $\bar{r} \sim T^{-1/4}$, both $\log\sigma_{sh}$ and $\log\Theta_{sh}$ are proportional to $T^{-1/4}$. The exponential in Θ_{sh}, $5\alpha\bar{r}/3$, is smaller than that in σ_{qq}, $8\alpha\bar{r}/3$, which explains the weaker temperature

dependence in Θ_{sh} than in σ_{qq}. As ϵ_0 decreases, which corresponds to an increase in the density of states at the Fermi level, $(\epsilon_0 a^3)^{-1}$, or the doping, T_0 will decrease, and consequently, both Θ_{sh} and σ_{qq} will increase and exhibit a weaker temperature dependence.

In summary, we have developed a theory of the SHE in disordered organic solids. The SHE is found to occur at the first order of SOC, due to misalignment of π-conjugated molecules in a disordered solid. We have numerically solved the transport equations in a large system and summed over all triads to obtain the spin Hall conductivity. The calculated values of the spin Hall angle and electrical conductivity are consistent with experimental measurements. Our theory suggests a tunable SHE in organic solids via their morphology.

This work was supported by the U.S. Army Research Office under Contract No. W911NF-15-1-0117.

[1] M. I. Dyakonov and V. I. Perel, Phys. Lett. **35A**, 459 (1971).
[2] See, e.g., G. Vignale, J. Supercond. Novel Magn. **23**, 3 (2010).
[3] K. Ando, S. Watanabe, S. Mooser, E. Saitoh, and H. Sirringhaus, Nat. Mater. **12**, 622 (2013).
[4] S. Watanabe, K. Ando, K. Kang, S. Mooser, Y. Vaynzof, H. Kurebayashi, E. Saitoh, and H. Sirringhaus, Nat. Phys. **10**, 308 (2014).
[5] V. Dediu, M. Murgia, F. C. Matacotta, C. Taliani, and S. Barbanera, Solid State Commun. **122**, 181 (2002).
[6] Z. H. Xiong, D. Wu, Z. V. Vardeny, and J. Shi, Nature (London) **427**, 821 (2004).
[7] Editorial, Nat. Mater. **8**, 691 (2009).
[8] T. Damker, H. Böttger, and V. V. Bryksin, Phys. Rev. B **69**, 205327 (2004).
[9] O. Entin-Wohlman, A. Aharony, Y. M. Galperin, V. I. Kozub, and V. Vinokur, Phys. Rev. Lett. **95**, 086603 (2005).
[10] G. F. Dresselhaus, Phys. Rev. **100**, 580 (1955).
[11] Yu. A. Bychkov and E. I. Rashba, J. Phys. C **17**, 6039 (1984).
[12] Z. G. Yu, Phys. Rev. Lett. **106**, 106602 (2011); Phys. Rev. B **85**, 115201 (2012).
[13] See Supplemental Material at http://link.aps.org/supplemental/10.1103/PhysRevLett.115.026601 for detailed derivations of Eqs. (1), (6), (7), and (13).
[14] Z. G. Yu, D. L. Smith, A. Saxena, R. L. Martin, and A. R. Bishop, Phys. Rev. Lett. **84**, 721 (2000); Phys. Rev. B **63**, 085202 (2001).
[15] T. Holstein, Phys. Rev. **124**, 1329 (1961).
[16] P. A. Bobbert, T. D. Nguyen, F. W. A. van Oost, B. Koopmans, and M. Wohlgenannt, Phys. Rev. Lett. **99**, 216801 (2007).
[17] Z. G. Yu, F. Ding, and H. Wang, Phys. Rev. B **87**, 205446 (2013).
[18] H. Böttger and V. V. Bryksin, *Hopping Conduction in Solids* (Akademie-Verlag, Berlin, 1985).
[19] P. N. Butcher and A. A. Kumar, Philos. Mag. B **42**, 201 (1980).
[20] A. M. Nardes, M. Kemerink, and R. A. J. Janssen, Phys. Rev. B **76**, 085208 (2007).
[21] N. F. Mott and E. A. Davis, *Electronic Processes in Non-Crystalline Materials* (Clarendon, Oxford, 1979).
[22] Z. G. Yu, Nat. Commun. **5**, 4842 (2014).
[23] J. J. Apperloo, R. A. J. Janssen, P. R. L. Malenfant, L. Groenendaal, and J. M. J. Fréchet, J. Am. Chem. Soc. **122**, 7042 (2000).
[24] S. S. Zade and M. Bendikov, J. Phys. Chem. C **111**, 10662 (2007).
[25] A. Miller and B. Abrahams, Phys. Rev. **120**, 745 (1960).
[26] J. M. Zhuo, L. H. Zhao, P. J. Chia, W. S. Sim, R. H. Friend, and P. K. H. Ho, Phys. Rev. Lett. **100**, 186601 (2008).
[27] G. T. Einevoll and C. A. Lütken, Phys. Rev. B **48**, 11492(R) (1993).